

## Response to Referee #1

We are once again thankful to the referee for her/his constructive comments. Please find below point by point response.

In response to my reviewer comment, the authors added a definition of "persistency" in their analysis which is very helpful. Still, I find the definition lacking in technical details. The authors state that "it is checked how many days back in time that particular wind direction was continuously sustained". This must involve some threshold of acceptable deviation. Were winds allowed to deviate by up to 10 degrees? 50 degrees? 1 degree? or did they truly need to be continuously sustained, to the same decimal point? This is of course a trivial detail, but I don't understand why it can't be included in their manuscript to help readers understand their exact approach. And how sensitive is their identification of "two distinct modes" to whatever threshold they chose?

The following text is added in the revised version to further clarify the definition of persistency.

"If an extreme event is observed, the wind speed and wind direction are computed for the last 10 days. It is then checked how many days back in time that particular wind direction was *continuously* sustained and that wind direction is not changed by more than  $\pm 15^\circ$  (a third of the quadrant) during that time period. It is to be noted that the choice of the  $\pm 15^\circ$  threshold is based on the visual inspection of about 25 test cases. It was found that if a stricter threshold is used (requiring wind direction deviations less than  $\pm 5^\circ$ ) the sampling is considerably reduced for long persistency events. On the other hand, if a more relax threshold is used (allowing deviations up to  $\pm 30^\circ$ ) we incorporate tail ends of the events that persisted over neighbouring areas."

The authors have added a sensitivity test based on cloud screening which is certainly helpful. Still, in their manuscript methods they state "we allowed retrievals under partially cloudy conditions to be analyzed" (this is repeated in Section 4). This statement is misleading, since it implies to me that there is some filtering that has been done ("partially cloudy"). Surely some scenes may be fully cloudy. The authors need to state explicitly that they have not applied any filter for cloudy data, and that they test the impact of this later.

The word "partially" is causing confusion here and hence it is removed from the text, now implying that all cases (irrespective of partly or fully cloudy conditions) were analysed.

I actually agree with Reviewer 2 regarding the question about the assumption that NO<sub>2</sub> observed from satellite is indicative of enhanced NO<sub>2</sub> levels on the ground. But I also agree with the authors that this is not necessarily within the scope of their current paper. However, I am a little disturbed that the author response is that they "put faith" in the datasets and "hope" the tropospheric columns would capture the variability near the ground. It is not the responsibility of the satellite retrieval science teams to guarantee the tropospheric columns have any relevance to surface conditions. It is also not the responsibility of the referee to point to references that discuss a discrepancy, as requested by the authors in response. Rather, in my opinion, it is the role of the authors to convince us that there isn't a discrepancy, or argue that any discrepancy is not important to their conclusions (which may very well be the case). Perhaps a compromise would be

for the authors to include a few comments/caveats to this point specifically, or to include references to other literature that supports any relevant assumptions.

We apologize for the poor choice of words and for not conveying the message properly. We do fully appreciate that in the end it is our responsibility to make sure that we use dataset properly for our purpose. The only point we wanted to make was that, as a user, we have gone through all relevant data documents and have tried to ensure that we use the data correctly. Since we are using retrievals only to select extreme events (rather than doing full scale transport analysis using retrievals) we thought our data handling should serve the purpose and that any validation work would be out of the scope of the present study.

We agree with the recent reviewer comment that the said discrepancy is not directly important for our work. This is because while characterizing meteorological conditions, we are interested in the enhanced NO<sub>2</sub> levels in the troposphere as a whole, not necessarily confined to the near-surface. In fact our study region could just be a part of the longer transit pathway for the eventual long-range transport of pollutants to the Arctic.

I commend the authors' approach to Figure 2, using monthly thresholds instead of seasonal thresholds. However, this figure is difficult to read. This could be corrected by simply including the absolute values of the 90th percentile for each month beside the legend labels. Also, why not label the colors by the month name, instead of a number (the rest of the plots refer to month names ("DJF", "SON", etc.)).

Figure 2 is revised. The months are labelled with names instead of numbers and corresponding 90th percentile thresholds are also added in brackets.

## Response to Referee #2

We are once again thankful to the referee for her/his constructive comments. Please find below point by point response.

The newly added sentences on page 11, line 51 do not look right to me - emissions are not given in ppb. Please check

Thanks. It is now corrected.

\* if I have not overlooked this information, the threshold for the cloud screening which was applied in the test case is not given. Please add.

The following sentence is now added to clarify it.

"We required that cloud fraction is less than 10% in AIRS data and valid retrievals of OMI cloud cleared tropospheric column NO<sub>2</sub> are available."

\* it would be really good to make Fig. 10 identical to Fig. 3 with respect to figure sizes and legend

Corrected.

\* I do not understand the sentence on page 14, line 163 "By definition, NO<sub>2</sub> anomalies during extreme events are similar in magnitude to climatological values over Scandinavia - please explain

Please note that we are referring to the anomalies (and not the absolute values).

\* page 14, line 153: concentrations => columns

Corrected.

\* There still are many small English issues which should be fixed before publication

We have tried to correct grammatical issues (in particular the use of articles).

1 **Typical meteorological conditions associated with extreme nitrogen dioxide**  
2 **(NO<sub>2</sub>) pollution events over Scandinavia**

3

4 Manu Anna Thomas and Abhay Devasthale

5

6 Research and development department, Swedish Meteorological and Hydrological Institute  
7 (SMHI), Folkborgsvägen 17, 60176 Norrköping, Sweden

8 Correspondence: manu.thomas@smhi.se

9

10 **Abstract**

11

12 Characterizing typical meteorological conditions associated with extreme pollution events  
13 helps in the better understanding of the role of local meteorology in governing the transport  
14 and distribution of pollutants in the atmosphere. The knowledge of their co-variability could  
15 further help to evaluate and constrain chemistry transport models (CTMs). Hence, in this  
16 study, we investigate the statistical linkages between extreme nitrogen dioxide (NO<sub>2</sub>)  
17 pollution events and meteorology over Scandinavia using observational and reanalysis data. It  
18 is observed that the south-westerly winds dominated during extreme events, accounting for  
19 50-65% of the total events depending on the season, while the second largest annual  
20 occurrence was from south-easterly winds, accounting for 17% of total events. The specific  
21 humidity anomalies showed an influx of warmer and moisture-laden air masses over  
22 Scandinavia in the free troposphere. Two distinct modes in the persistency of circulation  
23 patterns are observed. The first mode lasts for 1-2 days, dominated by south-easterly winds  
24 that prevailed during 78% of total extreme events in that mode, while the second mode lasted  
25 for 3-5 days, dominated by south-westerly winds that prevailed during 86% of the events. The  
26 combined analysis of circulation patterns, their persistency, and associated changes in  
27 humidity and clouds suggests that NO<sub>2</sub> extreme events over Scandinavia occur mainly due to  
28 the long-range transport from the southern latitudes.

## 29 1. Introduction

30

31 Nitrogen dioxide (NO<sub>2</sub>) is one of the highly reactive gases of the nitrogen oxides (NO<sub>x</sub>)  
32 family. The major sources of NO<sub>2</sub> are fuel combustion in motor vehicles, industrial boilers,  
33 emissions from soil and agricultural biomass burning. The natural source of NO<sub>2</sub> is lightning  
34 and forest fires. Recent studies indicate increasing trends in NO<sub>2</sub> in developing countries and  
35 decreasing trends in developed countries as a result of environmental regulation policies  
36 (Richter et al. 2005; Zhang et al. 2007; van der A et al. 2008; Schneider et al. 2015; Geddes et  
37 al. 2016). NO<sub>2</sub> is an oxidizing agent resulting in the corrosive nitric acid and plays an  
38 important role aiding the formation of ozone. It can also contribute to the formation of  
39 particulate matter (PM) and secondary organic particles through photochemical reactions.  
40 Increased NO<sub>x</sub> concentrations not only severely affect human physical health through reduced  
41 lung function, but also affect aquatic ecosystems through acid deposition and eutrophication  
42 of soil and water (Sjöberg et al. 2004; Klingberg et al. 2009; Bellandar et al. 2012; Gustafsson  
43 et al. 2014; Nilsson Sommar et al. 2014; Oudin et al. 2016; Taj et al. 2016). Lamarque et al.  
44 (2013) based on the multi-model intercomparison assessed increases in regional nitrogen  
45 deposition by up to 30-50% from RCP 2.6 to RCP 8.5. According to the 4th IPCC  
46 Assessment Report, the total global NO<sub>x</sub> emissions have increased from a pre-industrial value  
47 of 12 Tg N/yr to between 42 and 47 Tg N/yr in 2000. The most recent study by Miyazaki et  
48 al. (2017) estimated a ten year (2005-2014) global total surface NO<sub>x</sub> emissions of 48.4 Tg  
49 N/year with an increase of 29%, 26% and 20% per decade increase respectively over India,  
50 China and Middle East and a decrease of 38%, 8.2% and 8.8% respectively over United  
51 States, southern Africa and western Europe. In heavily polluted areas NO<sub>2</sub> can also have  
52 noticeable impact on the local radiation budget (Vasilkov et al. 2009).

53

54 Compared to other pollutants such as carbon monoxide (CO) that has a life span of weeks to  
55 few months, NO<sub>2</sub> has a relatively shorter life time in the atmosphere and ranges typically from  
56 a couple of hours in the boundary layer to up to few days in the upper troposphere (Beirle et  
57 al., 2011). Therefore, NO<sub>2</sub> can be typically associated with short-range transport events. For  
58 long range transport (LRT) or intercontinental transport of pollutants and in particular of NO<sub>2</sub>  
59 to occur, the associated weather systems need to be linked with stronger winds and rapid  
60 convective-advective events such as cyclones or warm conveyor belts (WCBs) that can lift air

61 masses from their source regions up into the free troposphere and be transported across the  
62 oceans (Eckhardt et al. 2003; Stohl et al. 2003). Due to lower concentrations of radical species  
63 in the free troposphere, the reaction with NO<sub>2</sub> is limited. Zien et al. (2014) identified about  
64 3800 LRT events of NO<sub>2</sub> during a 5 year period from the major pollution hotspots such as the  
65 east coast of North America, central Europe, China and South America, predominantly during  
66 autumn and winter months.

67

68 There have been several studies reporting individual LRT events of NO<sub>2</sub>. To mention a few,  
69 Stohl et al. (2003) in a study explained “intercontinental express highways” being responsible  
70 for almost 60% of the total intercontinental transport of pollutants from across the Atlantic to  
71 Europe, resulting in an increment of average European winter NO<sub>x</sub> mixing ratios by about 2-3  
72 pptv. In yet another study, Schaub et al. (2005) demonstrated that at least 50 % of the NO<sub>2</sub>  
73 recorded at the Alpine region was advected via a frontal system from the Ruhr area in central  
74 Germany in February 2001. Donnelly et al. (2015) reported that easterly air masses during  
75 winter resulted in increased NO<sub>2</sub> concentrations in the urban and rural sites in Ireland. LRT of  
76 NO<sub>x</sub> across the Indian Ocean from South Africa to Australia in May 1998 was reported by  
77 Wenig et al. (2003).

78

79 The Nordic countries often lie at the receiving end of short-range pollutant transport from  
80 northern Europe or they are a part of a much larger transit pathway of eventual long-range  
81 transport to the Arctic, originating from either Europe or North America. To what extent such  
82 a transport from the southerly latitudes affects the characteristics of extreme pollution events  
83 (such as magnitude, frequency and persistence) over Scandinavia depends largely on  
84 prevailing circulation patterns and meteorological conditions. The local meteorology can  
85 enhance or dampen the concentration of the pollutants depending on the degree of  
86 persistency; the knowledge of which would help to better constrain the chemistry transport  
87 models (CTMs). Therefore, identifying the dominant weather patterns over Scandinavia  
88 especially during extreme pollution is important. However, there has not been a systematic  
89 study linking the transport events of NO<sub>2</sub> to different meteorological conditions, solely from  
90 observational data over the Scandinavian region. Therefore, the main aim of the present study  
91 is to characterize circulation regimes and meteorological conditions extreme pollution events,  
92 to understand to what extent they differ from climatological conditions. There are two

93 different ways to study this co-variability solely using observational data: 1) the “top- down  
94 approach” wherein the atmospheric state is first identified and then the variability of the  
95 tracers is evaluated. This approach gives a general perspective of the distribution of tracers  
96 based on a particular weather state and 2) the “bottom-up approach” wherein the pollution  
97 episode is first identified and the weather state associated with it is studied. In this study we  
98 make use of the bottom-up approach as explained in the next section.

99

## 100 **2. Data sets and methodology**

101 The NO<sub>2</sub> tropospheric column densities from OMI (Ozone Monitoring Instrument) on board  
102 the EOS Aura satellite are used in this study to define and identify extreme events (Boersma  
103 et al., 2001, 2008, 2011; Bucsela et al., 2006, 2008, 2013; Lamsal et al. 2008, 2010, 2014). 11  
104 years (2004 – 2015) of daily Level 3 gridded standard product, available at 0.25x0.25 degrees  
105 resolution is analysed (OMNO2d, Version 3, available at:  
106 [https://disc.gsfc.nasa.gov/Aura/data-holdings/OMI/omno2d\\_v003.shtml](https://disc.gsfc.nasa.gov/Aura/data-holdings/OMI/omno2d_v003.shtml)). This particular  
107 product is used as it provides good quality OMI retrievals, already screened based on  
108 recommendations by the OMI Algorithm Team. **We allowed retrievals under cloudy**  
109 **conditions to be analysed**, not only to have robust number of samples, but also to avoid clear-  
110 sky biases since the NO<sub>2</sub> transport is often associated with cyclonic systems that lead to  
111 increased cloudiness (Zien et al. 2014). We further tested the sensitivity of our results to using  
112 only cloud screened retrievals, to evaluate if the selection of extreme events and associated  
113 meteorological conditions are different from those cases when retrievals under partially  
114 cloudy conditions are used.

115

116 Humidity and cloud fraction retrievals from the AIRS (Atmospheric Infrared sounder)  
117 instrument on board Aqua satellite are used (Chahine et al. 2006; Susskind et al. 2014;  
118 Devasthale et al. 2016). Both Aqua and Aura satellites are a part of NASA’s A-Train convoy,  
119 providing added advantage of simultaneous observations of trace gases from OMI-Aura and  
120 thermodynamical information from AIRS-Aqua. AIRS Version 6 Standard Level 3 Daily  
121 Product (AIRX3STD) for the same period (2004-2015) is used (data available at:  
122 <https://disc.gsfc.nasa.gov/uui/datasets?keywords=%22AIRS%22>).

123

124 To investigate circulation patterns, u and v wind components at 850 hPa from ECMWF's  
125 ERA-Interim Reanalysis are used (Dee et al., 2011;  
126 <http://apps.ecmwf.int/datasets/data/interim-full-daily/levtype=sfc/>).

127

128 In order to investigate co-variability of meteorological conditions and pollutants using  
129 observations, two different approaches can be taken (Fig. 1). In a “top-down” approach, a  
130 weather state classification can be done to identify most prevailing weather states that occur  
131 over the study area and then the relative distribution of pollutants can be investigated under  
132 those states to rank them. This approach was adapted by Thomas and Devasthale (2014) and  
133 Devasthale and Thomas (2012). In a “bottom-up” approach on the other hand, a set of  
134 pollution events can be identified first and then the corresponding meteorological conditions  
135 can be investigated. This bottom-up approach is the focus of the present study. It should be  
136 mentioned that both of these approaches have their advantages and limitations. For example,  
137 the dominant weather pattern identified in the top-down approach may not have the largest  
138 impact on pollutant variability and the pollution events identified in the bottom-up approach  
139 may not be associated with the dominant weather pattern or may not have the largest impact  
140 on an average in the weather state they occur. Therefore, only the combination of these two  
141 approaches will provide a complete picture of the co-variability between meteorological  
142 conditions and pollutants.

143

144 In the present study, an “extreme” pollution event is defined as follows. First, the histograms  
145 of NO<sub>2</sub> tropospheric column densities using OMI data for each month are computed over the  
146 centre of the study area (55N-60N, 11E-20E). This area is chosen because it accommodates  
147 top ten polluted and populated cities/regions in Sweden (Sjöberg et al. 2004; Klingberg et al.  
148 2009; Bellandar et al. 2012; Gustafsson et al. 2014; Nilsson Sommar et al. 2014; Oudin et al.  
149 2016; Taj et al. 2016 ). All events that surpass the 90-percentile (90%ile) value are considered  
150 as extreme events. The monthly histograms of NO<sub>2</sub> over the study region are shown in Fig. 2  
151 along with 90 percentile thresholds for each month (vertical lines). Since NO<sub>2</sub> distributions  
152 over the study area show strong monthly variability, the monthly thresholds were chosen to  
153 define extreme events. The distributions of NO<sub>2</sub> have longer tails during winter half year and  
154 the tropospheric columns are also higher. Therefore, the resulting 90%ile thresholds are also  
155 higher in winter compared to summer months. However, using thresholds based on

156 percentiles (rather than having a fixed value throughout the season or year), makes the criteria  
157 for the selection of extreme events fair and equally applicable for each month.

158

### 159 **3. Meteorological conditions observed during extreme events**

160

161 The spatial distribution of tropospheric NO<sub>2</sub> column during climatological conditions,  
162 extreme events and anomalies thereof is presented in Fig. 3. Note that although the thresholds  
163 for defining extreme events are different for each month, the results are compiled over four  
164 distinct seasons for the sake of brevity. By definition, NO<sub>2</sub> anomalies during extreme events  
165 are similar in magnitude to climatological values over Scandinavia. The spatial extent of the  
166 severity of the extreme pollutant episodes over southern Sweden is noticeable. Under  
167 climatological conditions, highest concentrations are observed over northern Germany and  
168 France, the Netherlands and Belgium (the Benelux region). There is a good spatial coherence  
169 between NO<sub>2</sub> distributions under climatological conditions and extreme events, in the sense  
170 that the high concentrations of NO<sub>2</sub> seemed to have spread over southern Scandinavia during  
171 extreme events from the regions where climatological values are usually higher. It is to be  
172 noted that during extreme events the pollution levels over northern European regions are also  
173 enhanced. For an event to qualify as an extreme event over southern Scandinavia, the  
174 pollutant levels in the source regions also need to be higher than usual in order to allow strong  
175 transport under favourable atmospheric circulation patterns. This provides confidence in the  
176 selection process of extreme events. The NO<sub>2</sub> concentrations are relatively higher in winter  
177 and autumn compared to the summer months. This is mainly because atmospheric removal by  
178 radical species and deposition are much more efficient in the summer months.

179

180 In order to characterize typical meteorological conditions that can result in such high  
181 concentrations over Scandinavia, we first investigated the dominant wind direction at 850 hPa  
182 associated with those extreme events using ERA-Interim reanalysis data. The normalized  
183 frequency of occurrence of different wind directions during four seasons is shown in Fig. 4. It  
184 can be seen that, irrespective of the season, the south-westerly winds are dominant during  
185 extreme events accounting for 50-65% of total events. This is consistent with south-westerly  
186 extension of pollution plume mentioned earlier. The second largest annual occurrence is from

187 south-easterly winds, accounting for 17% of total events followed equally similar contribution  
188 from north-westerly winds. Compared to climatological conditions, south-westerly winds  
189 have 30-40% more likelihood of being dominant during extreme events depending on the  
190 season. However, such clear tendency compared to climatological conditions is not observed  
191 in the case of other wind directions. The spatial pattern of the 850 hPa winds based on ERA-  
192 Interim reanalysis and corresponding humidity anomalies at 850 hPa based on AIRS data  
193 during extreme events are shown in Figs. 5 and 6 respectively. A clear transport pathway  
194 from the northern continental Europe to Scandinavia is visible. The strongest winds are  
195 observed during the DJF months followed by the SON months with average wind speeds  
196 reaching over 10 m/s. The weakest winds are observed during the JJA months. The circulation  
197 pattern is characterized by the presence of low pressure systems in the Norwegian Sea that  
198 create favourable conditions for the transport of pollutants from continental Europe into  
199 Scandinavia. The location of the center of these cyclonic systems can slightly vary over the  
200 Norwegian Sea, affecting the direction and strength of the northward flow, as evident in Fig.  
201 5. For example, in the DJF months, the center is located far away in the open Norwegian Sea  
202 allowing stronger south-westerly winds over southern Scandinavia. In the JJA months, the  
203 center of cyclonic systems is close to western Norwegian coast. While this pattern also leads  
204 to south-westerly winds, air masses are mixed with colder and drier air from the northern  
205 Norwegian Sea.

206

207 The specific humidity anomalies show an influx of warmer and moister air masses over  
208 Scandinavia (Fig. 6), except in summer as mentioned above. The seasonality in the vertical  
209 structure of the specific humidity anomalies over Scandinavia is shown in Fig. 7c. While there  
210 are large deviations in humidity anomalies, influenced by the strength of the wind flow, they  
211 are positive regardless of the season during extreme events and peak at 2-3 km above the  
212 surface. Such increase in the free tropospheric moisture, especially during winter half year in  
213 the absence of local moisture sources, can only be explained by the transport from southern  
214 latitudes. The vertical water vapour anomalies are higher in winter half year (DJF and SON),  
215 consistent with high NO<sub>2</sub> anomalies during those months. Fig. 8 further shows cloud fraction  
216 anomalies. Average cloudiness is increased in all seasons during extreme events, in particular  
217 during winter half year. During this time of year, the large-scale frontal systems originating  
218 from the southwesterly regions can bring moister airmasses over Scandinavia, as can be seen  
219 in the circulation patterns and humidity anomalies, creating favourable conditions for cloud

220 formation. Therefore, these positive cloud fraction anomalies, in combination with positive  
221 humidity anomalies and circulation patterns, are indicative of the long-range transport of  
222 airmasses associated with increased NO<sub>2</sub> concentrations.

223

224 For an extreme pollution event to be linked with the transport the wind flow should be  
225 stronger allowing rapid advection and associated circulation pattern also needs to be  
226 persistent. Fig. 7a and 7b show the histograms of wind speed at 850 hPa over the study areas  
227 during extreme events when data are partitioned by wind direction and by season respectively.  
228 The average values of wind speeds are also shown for extreme events and climatological  
229 conditions (in brackets). Although the distributions are shifted to higher wind speeds in nearly  
230 all cases during extreme events compared to climatological conditions, the average wind  
231 speeds are not significantly different. The south-westerly winds are strongest and show largest  
232 difference in average wind speeds, while the northeasterly winds are weakest. Average wind  
233 speeds during the winter half year (DJF and SON) are higher than the summer half year,  
234 consistent with observed positive anomalies of humidity and clouds.

235

236 The persistency of the different circulation patterns during these extreme events is further  
237 evaluated as shown in Fig. 7d. The persistency is defined as follows. **If an extreme event is  
238 observed, the wind speed and wind direction are computed for the last 10 days. It is then  
239 checked how many days back in time that particular wind direction was *continuously*  
240 sustained and that wind direction is not changed by more than  $\pm 15^{\circ}$  (a third of the quadrant)  
241 during that time period. It is to be noted that the choice of the  $\pm 15^{\circ}$  threshold is based on the  
242 visual inspection of about 25 test cases. It was found that if a stricter threshold is used  
243 (requiring wind direction deviations less than  $\pm 5^{\circ}$ ) the sampling is considerably reduced for  
244 long persistency events. On the other hand, if a more relax threshold is used (allowing  
245 deviations up to  $\pm 30^{\circ}$ ) we incorporate tail ends of the events that persisted over neighbouring  
246 areas.** Two distinct modes in the persistency of circulation patterns are observed, one in which  
247 a particular wind direction persists for a day or two and a second mode in which winds  
248 persists for 3 to 5 continuous days. This is clearly different from the degree of persistency  
249 observed under climatological conditions when winds persisted in one particular direction  
250 predominantly for few days. It was identified that during extreme events south-easterly winds  
251 dominated the first mode explaining 78% of the total occurrence in that mode and the

252 westerly winds dominated the second mode explaining 86% of the total occurrence. In the  
253 latter case, when the winds persist for few days (3-5 days), the conditions are favourable for  
254 the long-range transport from the southern latitudes since circulation patterns (Fig. 5) are  
255 associated with typical frontal systems and baroclinic disturbances that make their way over  
256 Scandinavia.

257

258

#### 259 **4. Sensitivity of chosen events to cloud clearing procedure**

260

261 As mentioned in Section 2, we allowed retrievals under cloudy conditions to be analysed, not  
262 only to have a robust number of samples, but also to avoid potential clear-sky biases.

263 However, clouds can contaminate the NO<sub>2</sub> retrievals by modulating scattering in the  
264 atmosphere. Moreover, clouds are highly variable not only in space and time but also in their  
265 nature, thus making it challenging to assess their overall impact on the quality of retrievals. In  
266 the case of our study, potential cloud contamination can affect the selection of extreme events  
267 and thereby associated weather patterns that are being studied. Therefore, we carried out a  
268 sensitivity study wherein the entire analysis was repeated using only cloud screened NO<sub>2</sub>  
269 retrievals to investigate to what extent cloud clearing would affect the chosen events and  
270 subsequent analysis. We required that cloud fraction is less than 10% in AIRS data and valid

271 retrievals of OMI cloud cleared tropospheric column NO<sub>2</sub> are available. Fig. 9 shows the  
272 histograms of NO<sub>2</sub> total columns under partially cloudy (solid lines) and cloud screened  
273 conditions (dotted lines). The histograms are accumulated over four seasons instead of  
274 months for clarity (to avoid too many lines). The chosen 90%ile thresholds are certainly  
275 different under partially cloudy and cloud screened conditions, but only slightly. We also  
276 found that, depending on the month, the selected extreme events match under partially cloudy  
277 and cloud screened conditions between 76% and 88% of the time. Fig. 10 further shows the  
278 spatial climatological distribution of NO<sub>2</sub> and during extreme events using only cloud  
279 screened retrievals. When compared to Fig. 3, the spatial distributions look patchy as a result  
280 of selected screening, but the magnitude and spatial features do not change significantly,  
281 providing confidence in our earlier analysis based on partially cloudy retrievals. Finally we  
282 evaluated if the events based on cloud screened data impact the analysis of meteorological

283 conditions investigated here. Fig. 11 shows the vertical structure of specific humidity  
284 anomalies over the study region under partially cloudy (solid lines) and cloud screened  
285 conditions (dotted lines). While the slight differences in the vertical structure do exist, their  
286 sign and magnitudes are not large enough to change any previous argumentation.

287

## 288 **5. Conclusions**

289

290 The main aim of the present study was to characterize typical meteorological conditions  
291 associated with extreme NO<sub>2</sub> pollution events over Scandinavia. To that end, the study  
292 employs the bottom-up approach, in contrast to top-down approach taken by Thomas and  
293 Devasthale (2014) to study statistical co-variability of weather states and pollutant  
294 distribution. Such detailed analysis characterizing circulation patterns and meteorological  
295 conditions involving more than 300 extreme pollution events identified using satellite data has  
296 not been done before over the Scandinavian region. It is observed that the south-westerly  
297 winds dominated during extreme events accounting for 50-65% of total events, while the  
298 second largest annual occurrence was from south-easterly winds, accounting for 17% of total  
299 events followed by an equally similar contribution from north-westerly winds. Wind speeds  
300 are generally higher during extreme events, but only slightly, making it challenging to  
301 delineate distinct circulation regimes under these events. For the first time, we investigated  
302 the degree of persistency of wind direction during extreme events. In contrast to  
303 climatological conditions, two distinct modes of persistency were found; first one lasting a  
304 day or so and dominated by winds from south-easterly direction and the other mode lasting 3  
305 to 5 days dominated by south-westerly and north-westerly winds. This information on the  
306 degree of persistency in conjunction with circulation patterns could be useful to identify  
307 extreme transport events. Further analysis of circulation patterns in combination with spatial  
308 distribution of humidity and its vertical structure suggest that these events occur as a result of  
309 long-range transport from southern latitudes, most likely from the northern parts of Germany  
310 and France, the Netherlands and Belgium. The analysis presented here provides information  
311 that can be used in the process oriented evaluation of chemistry transport models over  
312 Scandinavia.

313

314

## 315 **Acknowledgements**

316

317 We gratefully acknowledge OMI and AIRS Science Team and NASA GES DISC for  
318 providing data. The wind data from ERA-Interim reanalysis have been obtained from the  
319 ECMWF Data Server. MT acknowledges funding support from the Swedish Clean Air and  
320 climate research program of IVL (Swedish Environmental Research Institute). Both MT and  
321 AD acknowledge Swedish National Space Board (grants 84/11:1, 84/11:2, Dnr: 94/16).

322

## 323 **References**

324

325 Beirle, S., Boersma, K. F., Platt, U., Lawrence, M. G., and Wagner, T.: Megacity Emissions  
326 and Lifetimes of Nitrogen Oxides Probed from Space, *Science*, 333, 1737–1739,  
327 doi:10.1126/science.1207824, 2011.

328

329 Bellander T, Wichmann J, and Lind T., Individual Exposure to NO<sub>2</sub> in Relation to Spatial and  
330 Temporal Exposure Indices in Stockholm, Sweden: The INDEX Study. *PLoS ONE* 7(6):  
331 e39536. doi:10.1371/journal.pone.0039536, 2009.

332

333 Boersma, K. F., E. J. Bucsela, E. J. Brinksma, J. F. Gleason, NO<sub>2</sub>, OMI-EOS Algorithm  
334 Theoretical Basis Document: Trace Gas Algorithms: NO<sub>2</sub>, 4, 12-35, 2001.  
335 [http://eosps0.gsfc.nasa.gov/eos\\_homepage/for\\_scientists/atbd/docs/OMI/ATBD-OMI-04.pdf](http://eosps0.gsfc.nasa.gov/eos_homepage/for_scientists/atbd/docs/OMI/ATBD-OMI-04.pdf)

336

337 Boersma, K. F., Jacob, D. J., Bucsela, E. J., Perring, A. E., Dirksen, R., van der A, R. J.,  
338 Yantosca, R. M., Park, R. J., Wenig, M. O., and Bertram, T. H.: Validation of OMI  
339 tropospheric NO<sub>2</sub> observations during INTEX-B and application to constrain NO<sub>x</sub> emissions

340 over the eastern United States and Mexico, *Atmos. Environ.*, 42, 4480–  
341 4497, doi:10.1016/j.atmosenv.2008.02.004, 2008.

342

343 Boersma, K. F., Eskes, H. J., Dirksen, R. J., van der A, R. J., Veefkind, J. P., Stammes, P.,  
344 Huijnen, V., Kleipool, Q. L., Sneep, M., Claas, J., Leitão, J., Richter, A., Zhou, Y., and  
345 Brunner, D.: An improved tropospheric NO<sub>2</sub> column retrieval algorithm for the Ozone  
346 Monitoring Instrument, *Atmos. Meas. Tech.*, 4, 1905–1928, doi: 10.5194/amt-4-1905-2011,  
347 2011.

348

349 Bucsela, E. J., Celarier, E. A., Wenig, M. O., Gleason, J. F., Veefkind, J. P., Boersma, K. F.,  
350 and Brinksma, E. J.: Algorithm for NO<sub>2</sub> vertical column retrieval from the ozone monitoring  
351 instrument, *IEEE T. Geosci. Remote*, 44, 1245–1258, doi:10.1109/TGRS.2005.863715, 2006.

352

353 Bucsela, E. J., Perring, A. E., Cohen, R. C., Boersma, K. F., Celarier, E. A., Gleason, J. F.,  
354 Wenig, M. O., Bertram, T. H., Wooldridge, P. J., Dirksen, R., and Veefkind, J. P.:  
355 Comparison of tropospheric NO<sub>2</sub> from in situ aircraft measurements with near-real-time and  
356 standard product data from OMI, *J. Geophys. Res.*, 113, D16S31, doi:10.1029/2007JD008838,  
357 2008.

358

359 Bucsela, E. J., Krotkov, N. A., Celarier, E. A., Lamsal, L. N., Swartz, W. H., Bhartia, P. K.,  
360 Boersma, K. F., Veefkind, J. P., Gleason, J. F., and Pickering, K. E.: A new stratospheric and  
361 tropospheric NO<sub>2</sub> retrieval algorithm for nadir-viewing satellite instruments: applications to  
362 OMI, *Atmos. Meas. Tech.*, 6, 2607-2626, doi:10.5194/amt-6-2607-2013, 2013.

363

364 Chahine, M. T and co-authors, AIRS: Improving Weather Forecasting and Providing New  
365 Data on Greenhouse Gases, *Bull. Am. Meteorol. Soc.*, 87, 911–926, 2006.

366

367 Dee, D. P., Uppala, S. M., Simmons, A. J., Berrisford, P., Poli, P., Kobayashi, S., Andrae, U.,  
368 Balmaseda, M. A., Balsamo, G., Bauer, P., Bechtold, P., Beljaars, A. C. M., van de Berg, L.,  
369 Bidlot, J., Bormann, N., Delsol, C., Dragani, R., Fuentes, M., Geer, A. J., Haimberger, L.,  
370 Healy, S. B., Hersbach, H., Hólm, E. V., Isaksen, L., Kållberg, P., Köhler, M., Matricardi, M.,  
371 McNally, A. P., Monge-Sanz, B. M., Morcrette, J.-J., Park, B.-K., Peubey, C., de Rosnay, P.,  
372 Tavolato, C., Thépaut, J.-N. and Vitart, F.: The ERA-Interim reanalysis: configuration and  
373 performance of the data assimilation system. *Q.J.R. Meteorol. Soc.*, 137: 553–597,  
374 doi:10.1002/qj.828, 2011.

375

376 Devasthale, A. and M. A. Thomas, An investigation of statistical link between inversion  
377 strength and carbon monoxide over Scandinavia in winter using AIRS data, *Atmospheric*  
378 *Environment*, Vol. 56, 109-114 s, DOI: 10.1016/j.atmosenv.2012.03.042, 2012.

379

380 Devasthale et al. A decade of space borne observations of the Arctic atmosphere: novel  
381 insights from NASA's Atmospheric Infrared Sounder (AIRS) instrument. *Bull. Amer. Meteor.*  
382 *Soc.* doi:10.1175/BAMS-D-14-00202.1, in press, 2016.

383

384 Donnelly, A. A., Broderick, B. M. and Misstear, B. D.: The effect of long-range air mass  
385 transport pathways on PM10 and NO2 concentrations at urban and rural background sites in  
386 Ireland: Quantification using clustering techniques, *J Environ Sci Health A Tox Hazard Subst*  
387 *Environ Eng.*, doi: 10.1080/10934529.2015.1011955, 2015.

388

389 Eckhardt, S., A. Stohl, S. Beierle, N. Spichtinger, P. James, C. Forster, C. Junker, T. Wagner,  
390 U. Platt, and S. G. Jennings, 2003: The North Atlantic Oscillation controls air pollution  
391 transport to the Arctic, *Atmos. Chem. Phys.*, 3, 1769-1778, 2003.

392

393 Ehhalt, D. H., Rohrer, F., and Wahner, A.: Sources and Distribution of NO<sub>x</sub> in the Upper  
394 Troposphere at Northern Mid-Latitudes, *J. Geophys. Res.*, 97, 3725–3738,  
395 <http://www.agu.org/journals/jd/v097/iD04/91JD03081/>, 1992.

396

397 Geddes JA, et al. Long-term trends worldwide in ambient NO<sub>2</sub> concentrations inferred from  
398 satellite observations. *Environ Health Perspect* 1243281–289.2892016,  
399 doi:10.1289/ehp.1409567, 2016.

400

401 Gustafsson, M., H. Orru, B. Forsberg, S. Åström, H. Tekie, K. Sjöberg, Quantification of  
402 population exposure to NO<sub>2</sub>, PM<sub>2.5</sub> and PM<sub>10</sub> in Sweden 2010, Swedish Environmental  
403 Research Institute (IVL), IVL Report B2197, pp. 74, December 2014.

404

405 Klingberg, J., M. P. Björkman, G. P. Karlsson, and H. Pleijel, Observations of Ground-level  
406 Ozone and NO<sub>2</sub> in Northernmost Sweden, Including the Scandian Mountain Range, *AMBIO*,  
407 38(8):448-451. doi: <http://dx.doi.org/10.1579/0044-7447-38.8.448>, 2009.

408

409 Lamarque, J.-F. and Dentener, F. and McConnell, J. and Ro, C.-U. and Shaw, M. and Vet, R.  
410 and Bergmann, D. and Cameron-Smith, P. and Dalsoren, S. and Doherty, R. and Faluvegi, G.  
411 and Ghan, S. J. and Josse, B. and Lee, Y. H. and MacKenzie, I. A. and Plummer, D. and  
412 Shindell, D. T. and Skeie, R. B. and Stevenson, D. S. and Strode, S. and Zeng, G. and Curran,  
413 M. and Dahl-Jensen, D. and Das, S. and Fritzsche, D. and Nolan, M., Multi-model mean  
414 nitrogen and sulfur deposition from the Atmospheric Chemistry and Climate Model  
415 Intercomparison Project (ACCMIP): evaluation of historical and projected future changes,  
416 *Atmos. Chem. Phys.*, 13, 7997-8018,2013.

417

418 Lamsal LN, Martin RV, van Donkelaar A, Celarier EA, Bucsela EJ, Boersma KF, et al.  
419 Indirect validation of tropospheric nitrogen dioxide retrieved from the OMI satellite  
420 instrument: insight into the seasonal variation of nitrogen oxides at northern midlatitudes. *J*  
421 *Geophys Res* 115D05302; doi:10.1029/2009JD013351 , 2010.

422

423 Lamsal LN, Martin RV, van Donkelaar A, Steinbacher M, Celarier EA, Bucsela E, et al.  
424 Ground-level nitrogen dioxide concentrations inferred from the satellite-borne Ozone  
425 Monitoring Instrument. *J Geophys Res* 113D16308; .10.1029/2007JD009235, 2008.

426

427 Lamsal, L. N., Krotkov, N. A., Celarier, E. A., Swartz, W. H., Pickering, K. E., Bucsela, E. J.,  
428 Gleason, J. F., Martin, R. V., Philip, S., Irie, H., Cede, A., Herman, J., Weinheimer, A.,  
429 Szykman, J. J., and Knepp, T. N.: Evaluation of OMI operational standard NO<sub>2</sub> column  
430 retrievals using in situ and surface-based NO<sub>2</sub> observations, *Atmos. Chem. Phys.*, 14, 11587-  
431 11609, doi:10.5194/acp-14-11587-2014, 2014.

432 Miyazaki, K. and Eskes, H. and Sudo, K. and Boersma, K. F. and Bowman, K. and Kanaya,  
433 Y., Decadal changes in global surface NO<sub>x</sub> emissions from multi-constituent satellite data  
434 assimilation, *Atmos. Chem. Phys.*, 17, 2017, 807-837, doi:10.5194/acp-17-807-2017.

435 Nilsson Sommar, J., A. Ek, R. Middelvel, A. Bjerg, S-E. Dahlén, C. Janson, B. Forsberg,  
436 Quality of life in relation to the traffic pollution indicators NO<sub>2</sub> and NO<sub>x</sub>: results from the  
437 Swedish GA2LEN survey, *BMJ Open Res* 2014;1:1 e000039 doi:10.1136/bmjresp-  
438 2014-000039.

439

440 Oudin, A., L. Bråbäck, D. Oudin Åström, M. Strömgren, and B. Forsberg, Association  
441 between neighbourhood air pollution concentrations and dispensed medication for psychiatric  
442 disorders in a large longitudinal cohort of Swedish children and adolescents, *BMJ Open*  
443 2016;6:6 e010004 doi:10.1136/bmjopen-2015-010004, 2016.

444

445 Richter A, Burrows JP, Nüss H, Granier C, Niemeier U. Increase in tropospheric nitrogen  
446 dioxide over China observed from space. *Nature* 437129–132.132; doi:10.1038/nature04092,  
447 2005.

448

449 Schneider, P., Lahoz, W. A., and van der A, R.: Recent satellite-based trends of tropospheric  
450 nitrogen dioxide over large urban agglomerations worldwide, *Atmos. Chem. Phys.*, 15, 1205-  
451 1220, doi:10.5194/acp-15-1205-2015, 2015.

452

453 Sjöberg K., M. Haeger-Eugensson, M. Lijeberg, H. Blomgren, and B. Forsberg,  
454 Quantification of population exposure to nitrogen dioxide in Sweden, Swedish Environmental  
455 Research Institute (IVL), IVL Report B1579, pp. 31, September 2004.

456

457 Stohl, A., Huntrieser, H., Richter, A., Beirle, S., Cooper, O. R., Eckhardt, S., Forster, C.,  
458 James, P., Spichtinger, N., and Wenig, M.: Rapid intercontinental air pollution transport  
459 associated with a

460 meteorological bomb, *Atmos. Chem. Phys.*, 3, 969–985, 2003, [http://www.atmos-chem-](http://www.atmos-chem-phys.net/3/969/2003/)  
461 [phys.net/3/969/2003/](http://www.atmos-chem-phys.net/3/969/2003/).

462

463 Schaub, D., Weiss, A. K., Kaiser, J. W., Petritoli, A., Richter, A., Buchmann, B., and  
464 Burrows, J. P.: A transboundary transport episode of nitrogen dioxide as observed from  
465 GOME and its impact in the Alpine region, *Atmos. Chem. Phys.*, 5, 23–37, doi:10.5194/acp-  
466 5-23-2005, 2005.

467

468 Susskind, J., J. M. Blaisdell and L. Iredell, Improved methodology for surface and  
469 atmospheric soundings, error estimates and quality control procedures: the atmospheric  
470 infrared sounder science team version-6 retrieval algorithm, *J. Appl. Remote Sens.*, 8(1),  
471 084994, doi:10.1117/1.JRS.8.084994, 2014.

472

473 Taj T, Stroh E, Åström DO, Jakobsson K, Oudin A., Short-Term Fluctuations in Air Pollution  
474 and Asthma in Scania, Sweden. Is the Association Modified by Long-Term Concentrations?  
475 PLoS ONE 11(11): e0166614. doi:10.1371/journal.pone.0166614, 2016.

476

477 Thomas, M. A. and Devasthale, A.: Sensitivity of free tropospheric carbon monoxide to  
478 atmospheric weather states and their persistency: an observational assessment over the Nordic  
479 countries, *Atmos. Chem. Phys.*, 14, 11545-11555, doi:10.5194/acp-14-11545-2014, 2014.

480

481 van der A, R. J., H. J. Eskes, K. F. Boersma, T. P. C. van Noije, M. Van Roozendaal, I. De  
482 Smedt, D. H. M. U. Peters, and E. W. Meijer, Trends, seasonal variability and dominant NO<sub>x</sub>  
483 source derived from a ten year record of NO<sub>2</sub> measured from space, *J. Geophys. Res.*, 113,  
484 D04302, doi:10.1029/2007JD009021, 2008.

485

486 Vasilkov, A. P., Joiner, J., Oreopoulos, L., Gleason, J. F., Veeffkind, P., Bucsele, E., Celarier,  
487 E. A., Spurr, R. J. D., and Platnick, S.: Impact of tropospheric nitrogen dioxide on the  
488 regional radiation budget, *Atmos. Chem. Phys.*, 9, 6389-6400, doi:10.5194/acp-9-6389-2009,  
489 2009.

490

491 Wenig, M., Spichtinger, N., Stohl, A., Held, G., Beirle, S., Wagner, T., Jähne, B., and Platt,  
492 U.: Intercontinental transport of nitrogen oxide pollution plumes, *Atmos. Chem. Phys.*, 3,  
493 387–393,

494 doi:10.5194/acp-3-387-2003, 2003.

495

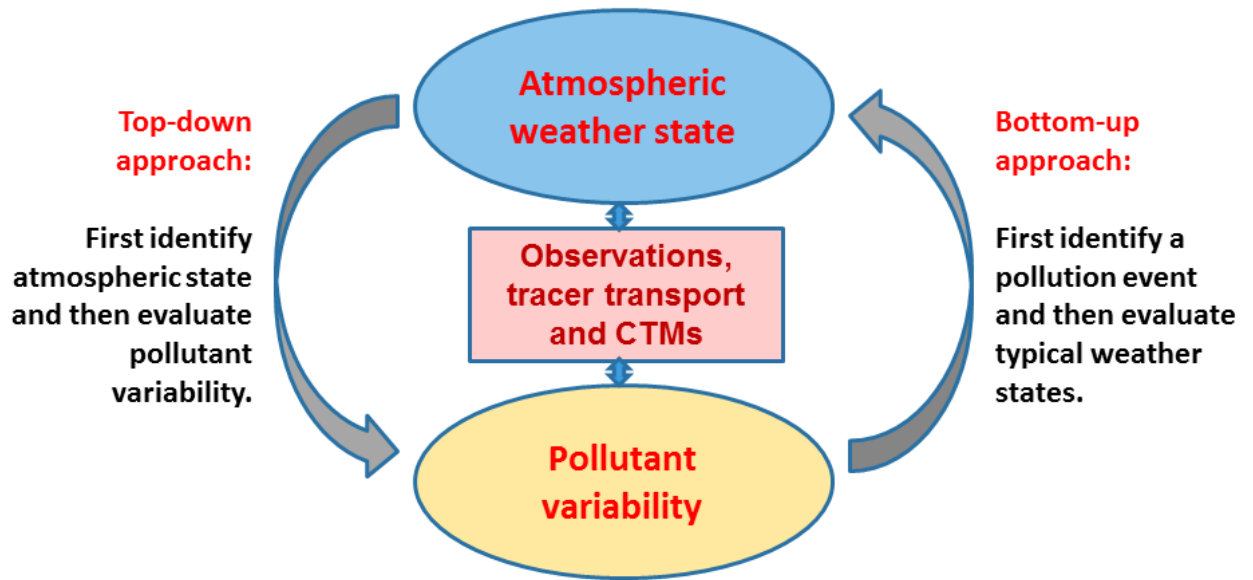
496 Zhang, Q., et al., NO<sub>x</sub> emission trends for China, 1995–2004: The view from the ground and  
497 the view from space, *J. Geophys. Res.*, 112, D22306, doi:10.1029/2007JD008684, 2007.

498

499 Zien, A. W., Richter, A., Hilboll, A., Blechschmidt, A.-M., and Burrows, J. P.: Systematic  
500 analysis of tropospheric NO<sub>2</sub> long-range transport events detected in GOME-2 satellite data,  
501 *Atmos. Chem. Phys.*, 14, 7367–7396, doi: 10.5194/acp-14-7367-2014, 2014.

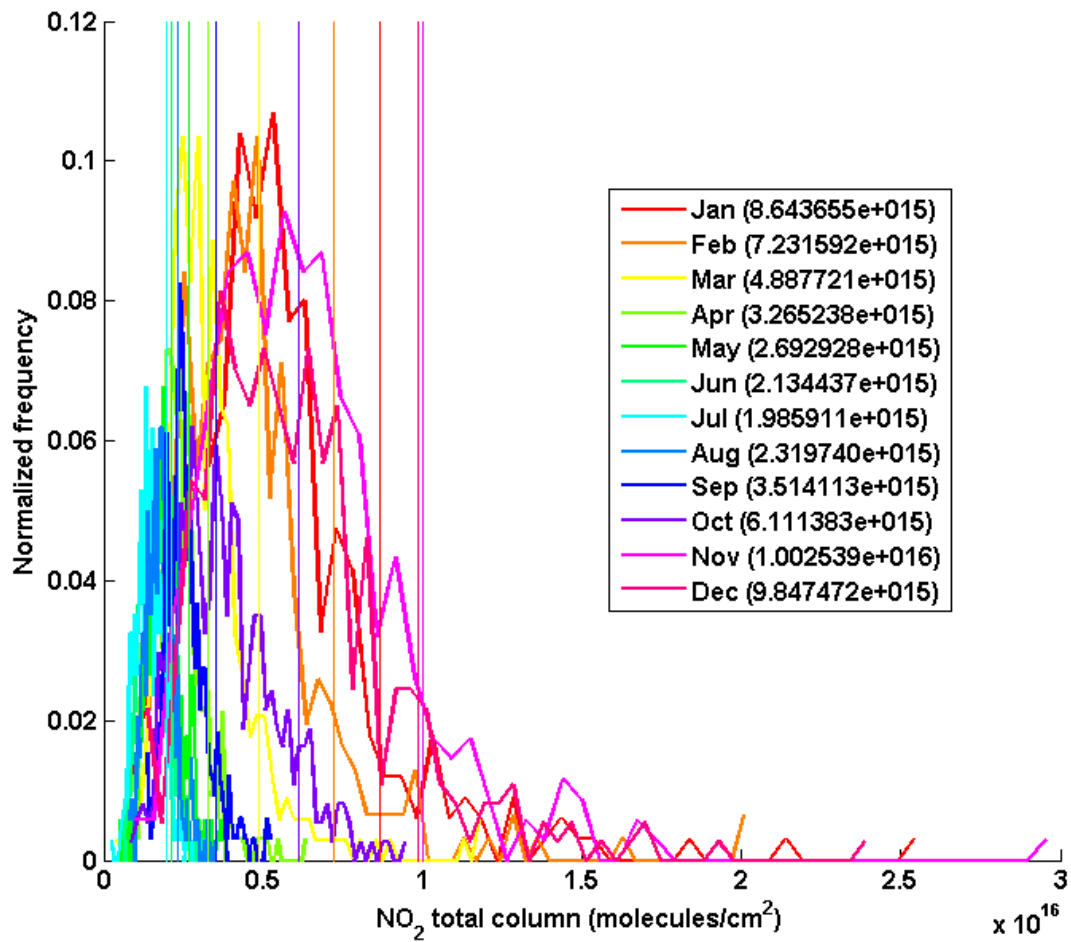
502

503



506 Fig. 1: Schematic showing two different approaches to study statistical co-variability of  
507 atmospheric weather states and pollutant concentrations.

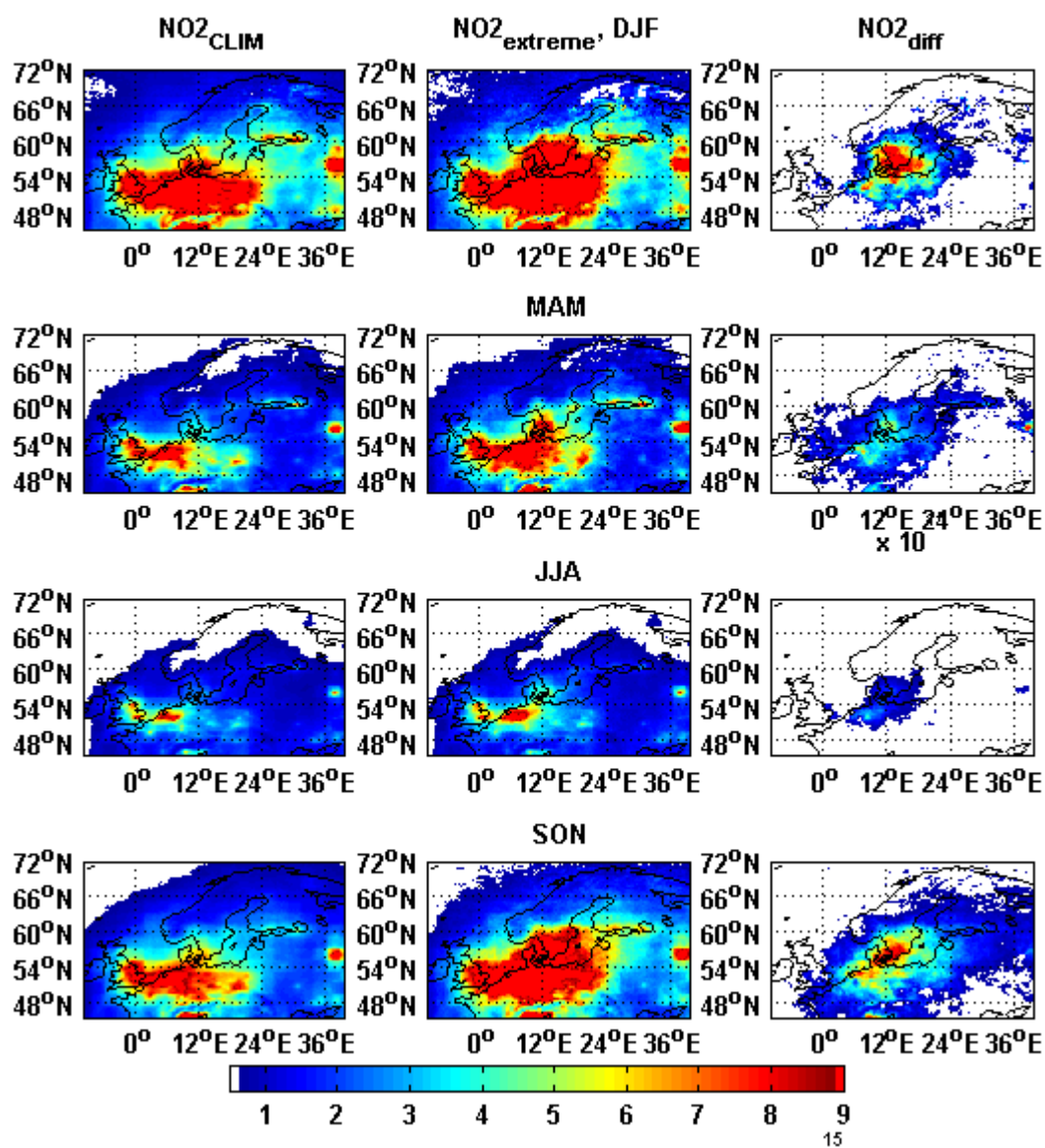
516



517

518 Fig. 2: Monthly histograms of tropospheric total column NO<sub>2</sub> over the centre of the study area  
519 (55N60N, 11E-20E) and corresponding 90%ile thresholds (shown by vertical lines, values in  
520 brackets).

521



522

523

524 Fig, 3: Seasonal, climatological average tropospheric NO<sub>2</sub> total column (first column) based  
 525 on nearly 11-yr OMI data (2004-2015), NO<sub>2</sub> distribution during extreme events (second  
 526 column) and the difference between the two (third column). The units are in molecules/cm<sup>2</sup>.

527

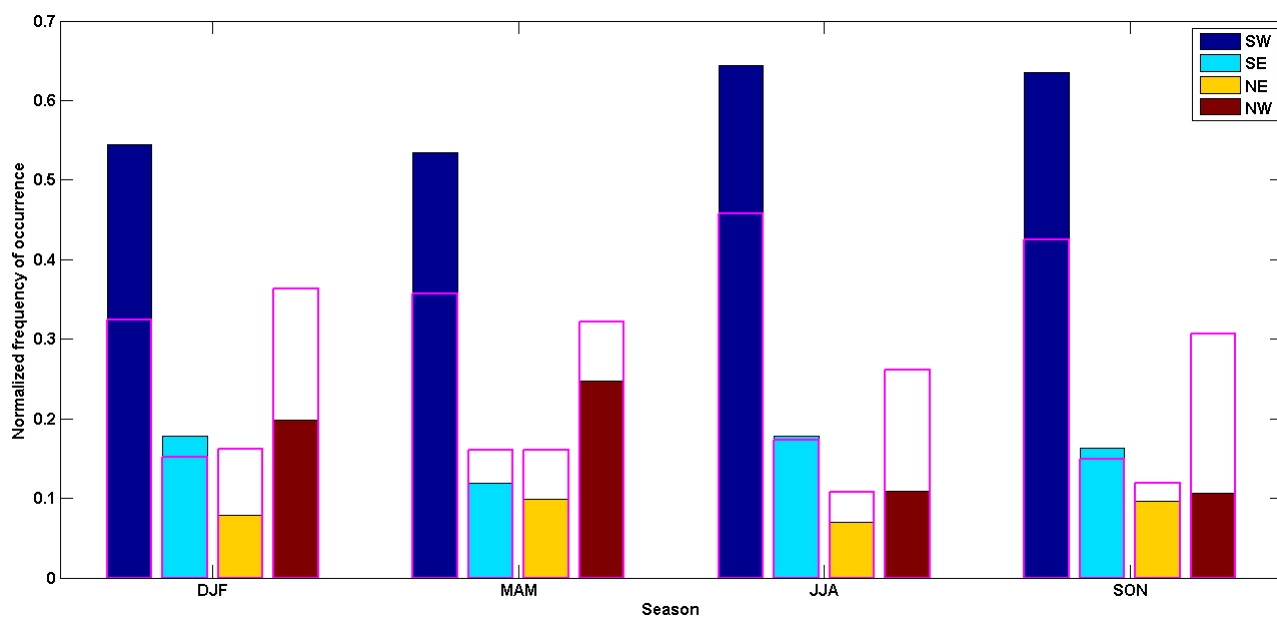
528

529

530

531

532



533

534

535

536 Fig. 4: Seasonal normalized frequency of occurrence of a particular wind direction at 850 hPa  
537 when NO<sub>2</sub> extreme pollution events were observed. The hollow magenta bars show  
538 normalized frequency under climatological conditions.

539

540

541

542

543

544

545

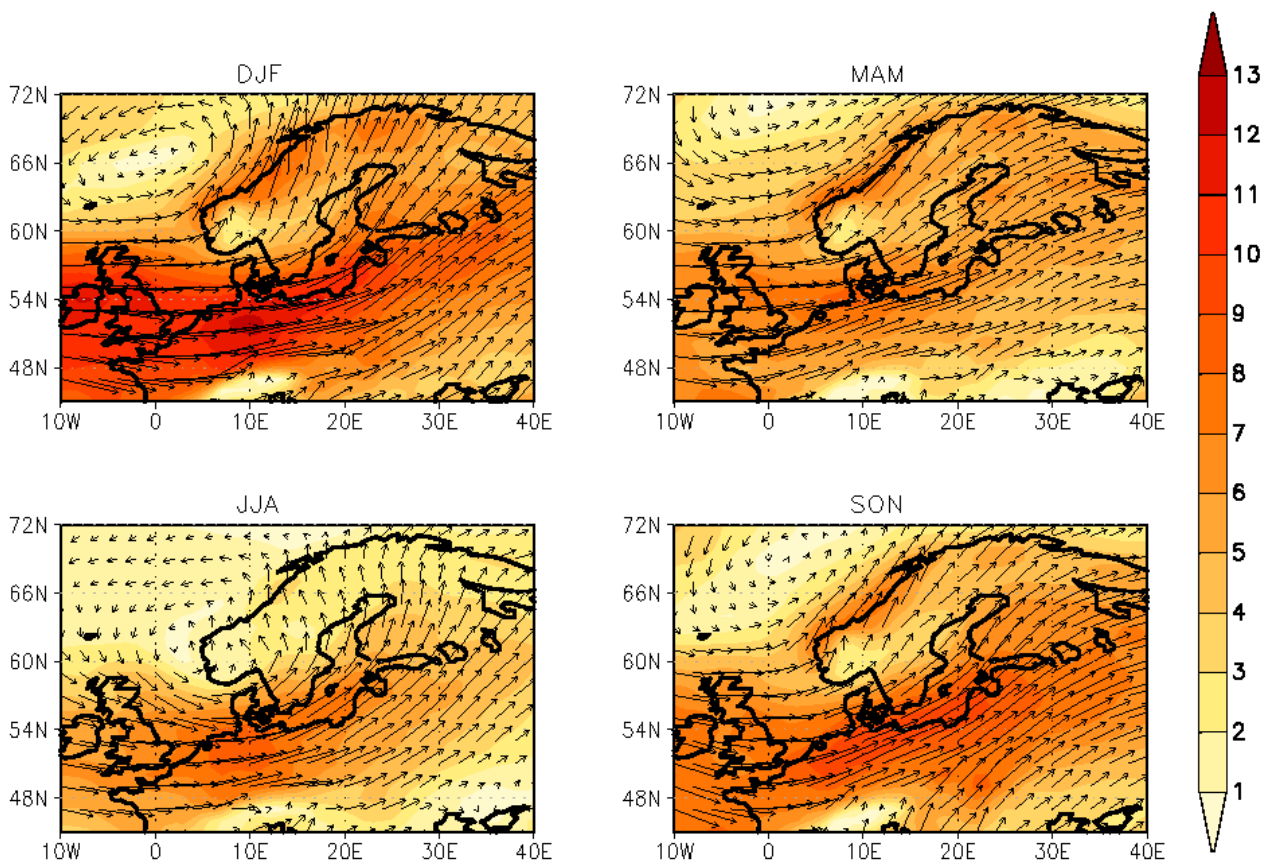
546

547

548

549

550



551

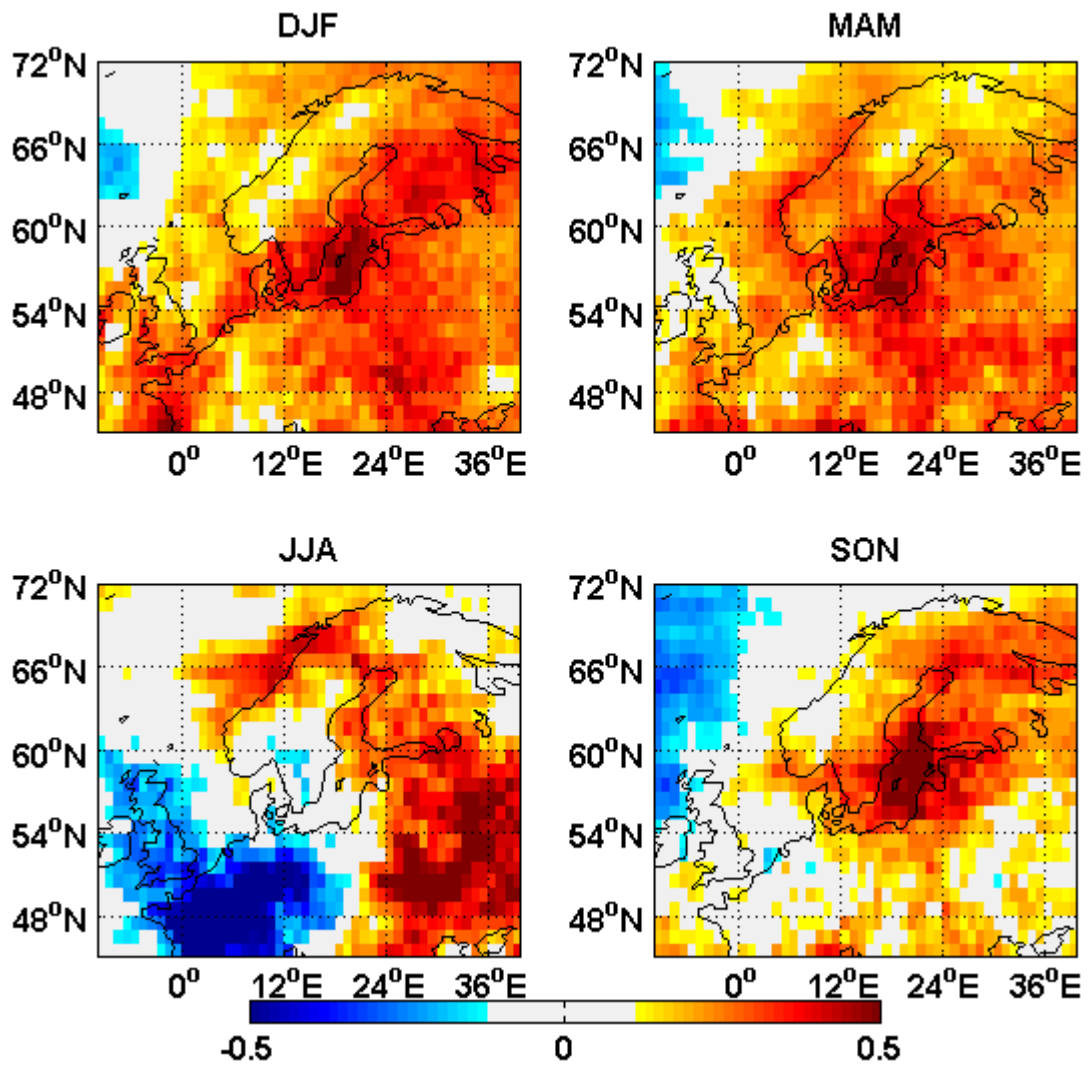
552

553

554

555 Fig. 5: Seasonal average wind strengths and direction at 850 hPa showing dominant  
556 circulation pattern observed when NO<sub>2</sub> extreme pollution events occur.

557



558

559

560 Fig. 6: The seasonal spatial patterns of specific humidity anomalies (g/kg) during extreme  
 561 NO<sub>2</sub> pollution events.

562

563

564

565

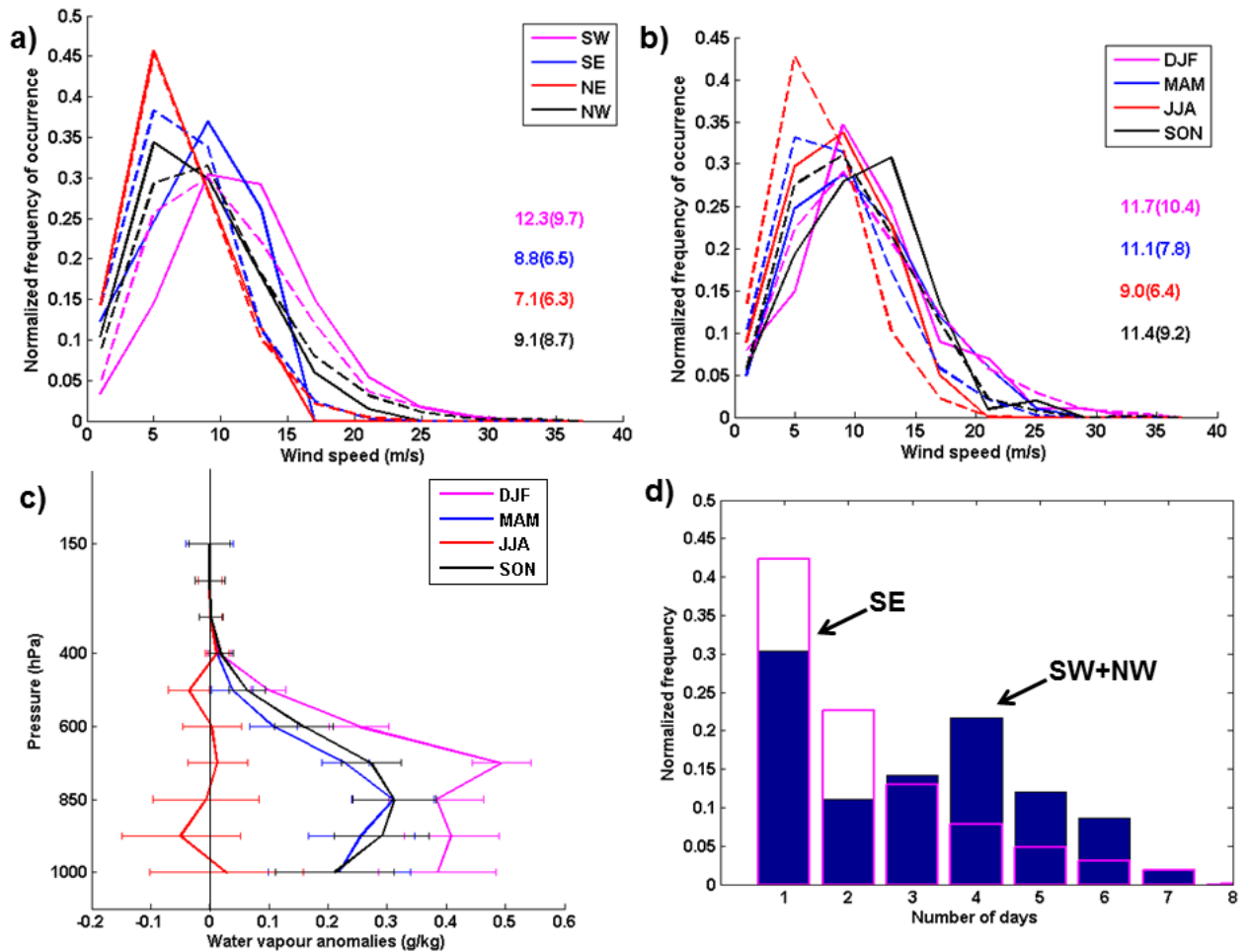
566

567

568

569

570



571

572

573 Fig. 7: a) Histograms of wind speeds (m/s) at 850 hPa over the center of the study area (55N-

574 60N, 11E-20E) during extreme events (solid lines) and climatological conditions (dotted

575 lines, 2004-2015) when data are partitioned for different wind directions. The numbers show

576 average wind speeds (m/s) during extreme events and in brackets under climatological

577 conditions. b) Same as in (a), but when wind data are partitioned for different seasons. c)

578 Vertical anomalies of specific humidity (g/kg) during extreme events with horizontal bars

579 showing standard deviations. d) Persistency of wind directions as a function of number of

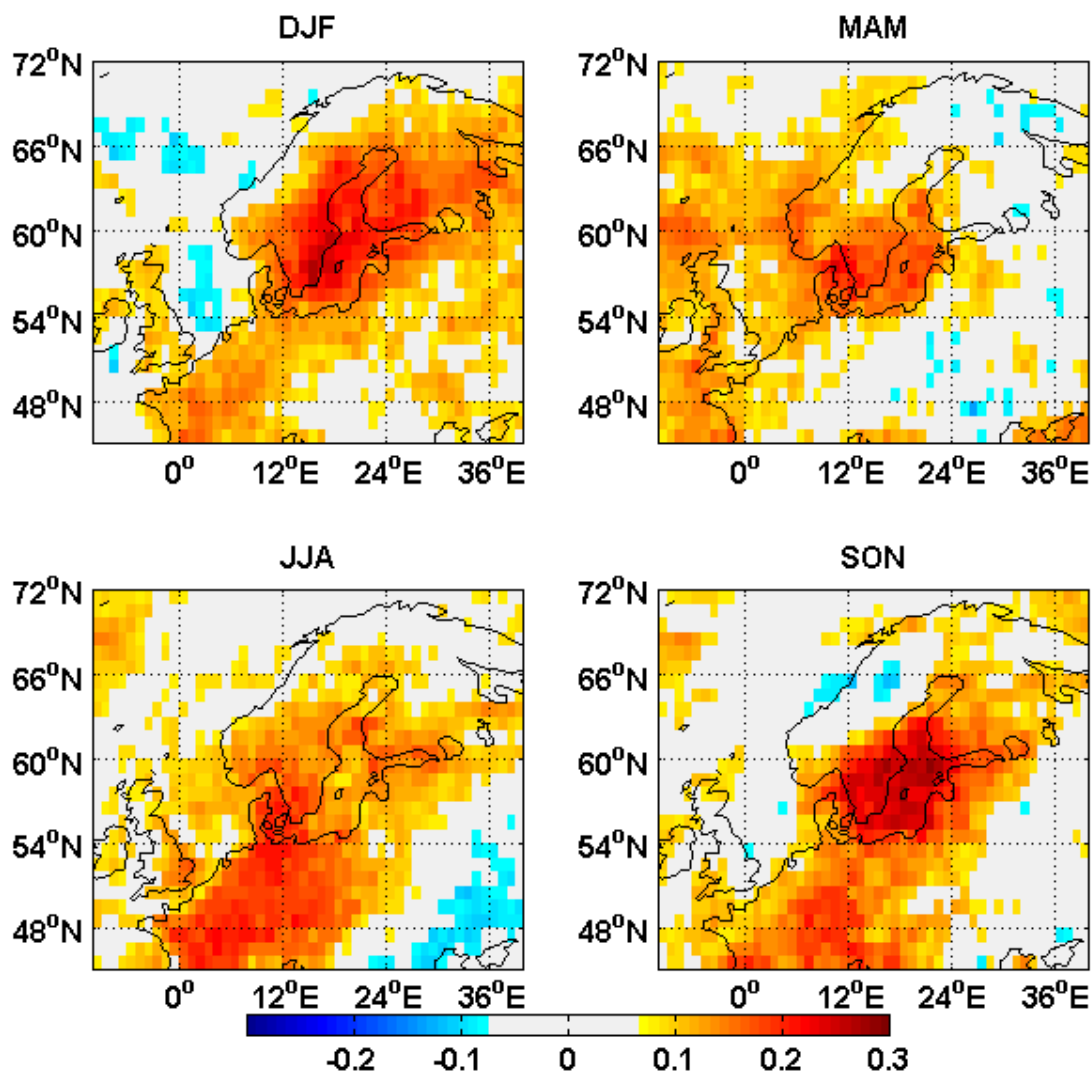
580 continuous days. The magenta bars show persistency under climatological conditions.

581

582

583

584



585

586

587 Fig. 8: Total cloud fraction anomalies observed during extreme events based on AIRS data.

588

589

590

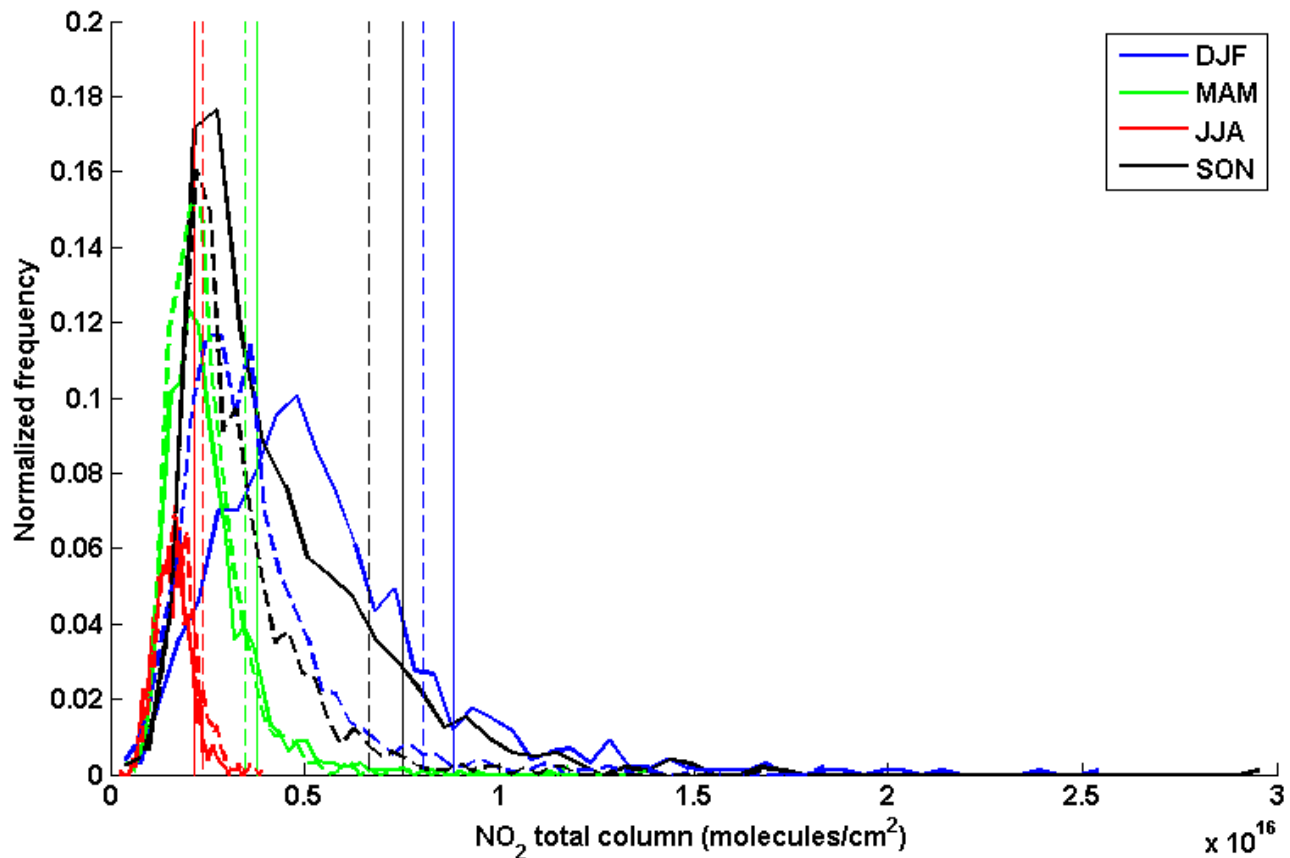
591

592

593

594

595



596

597

598 Fig. 9: Seasonal histograms of total column tropospheric NO<sub>2</sub> over the centre of the study area  
599 (55N-60N, 11E-20E) and corresponding 90%ile thresholds (shown by vertical lines). The  
600 solid lines show histograms based on retrievals under partially cloudy conditions, while the  
601 dotted lines show histograms based only on cloud cleared retrievals.

602

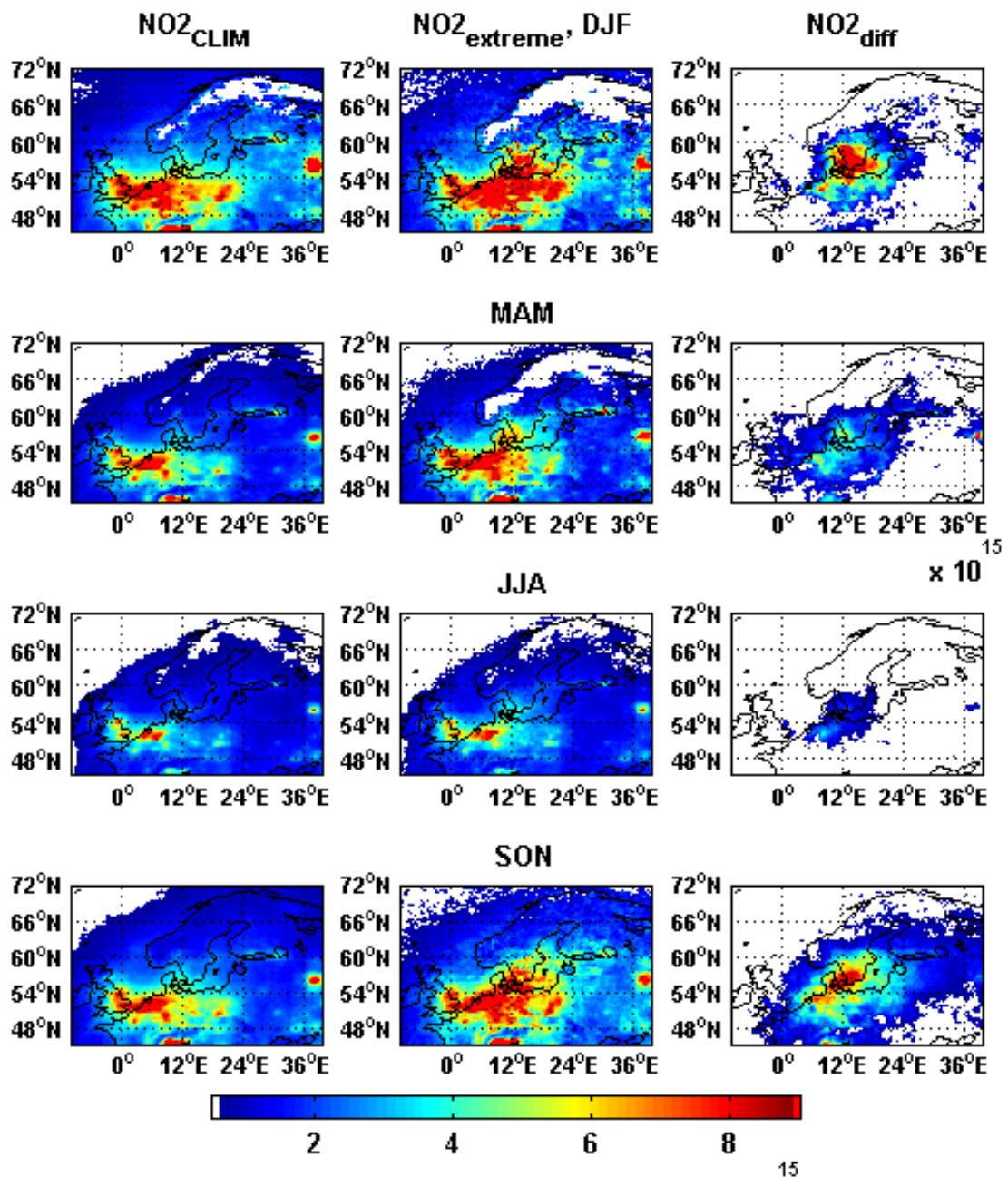
603

604

605

606

607



608

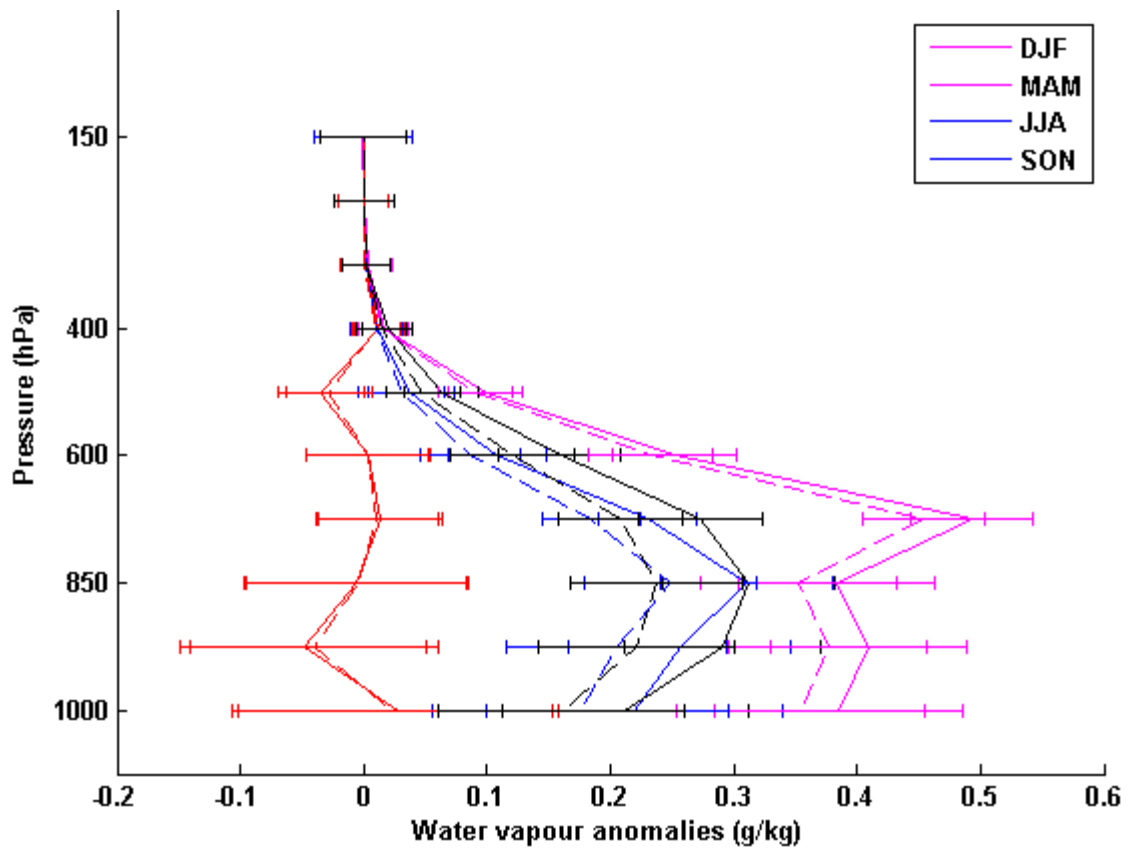
609 Fig. 10: Seasonal, climatological average tropospheric NO<sub>2</sub> total column (first column) based  
 610 only on cloud screened OMI data (2004-2015), NO<sub>2</sub> distribution during extreme events  
 611 (second column, also based on cloud screened data) and the difference between the two (third  
 612 column). The units are in molecules/cm<sup>2</sup>.

613

614

615

616



617

618

619 Fig. 11: Vertical anomalies of specific humidity (g/kg) during extreme events with horizontal  
620 bars showing standard deviations. The solid lines show anomalies under partially cloudy  
621 retrievals and dotted lines based on cloud screened retrievals.

622

623